A video compression algorithm for ATM networks with ABR service, using visual criteria

S. Felici, J. Martinez [1]

Institut de Robotica. Universitat de Valencia

Ph: +34 6 364 22 53 Fax: +34 6 364 48 41 Email:Santiago.Felici@uv.es

[1] Dept. Comunicaciones UPV

TOPICS: adaptive video compression algorithm, Rate-Distortion, multiresolution, biorthogonal wavelet transform, perceptual bit allocation, ATM-ABR services

Abstract: The design of adaptive video compression algorithms to support multimedia applications that can adapt to changing network conditions is currently being the subject of intense study. These applications do not require a guarantee QoS and their users are willing to pay less for just an acceptable quality. These applications are typically supported by best-effort *network services. One of these network services is the Available Bit Rate (ABR) service, which allocates the available bandwidth on the network to its users, via a closed-loop feedback control mechanism. The ABR sources can therefore adapt faster to new network conditions, achieving in this way less queueing delay and cell-loss rates. In addition, the ABR service allows the video sources to negotiate a Minimum Cell Rate (MCR) at connection set-up. This MCR can be dimensioned to achieve a minimum visual quality.*

In this paper [1] *we present an adaptive video compression algorithm specifically design for the transmission of video signals over an ABR connection. It is based on a 3D subband coding that uses wavelet filter banks but Does not use motion estimation. Motion estimation, which is common in video standards (H.261, H.263, MPEG-1, MPEG-2, etc), is not adequate for the transmission of video over connection offering a* best-effort *service, due to the error propagation effect.*

The proposed algorithm tries to minimise the impact that cell losses could have on the perceived quality, using perceptual bit allocation procedures and Rate-Distortion minimisation techniques. The algorithm estimates the rate at which the signal should be generated by means of a forecast mechanism based on the value of the feedback signal sent by the network. The Distortion is minimised using a subband priority scheme based on a Human Visual System (HVS) and taking into account the perceptual criteria. Some experimental results are also provided to show that a good performance can be obtained even under heavy network congestion situations.

1 Introduction

A new generation of systems called Networked Multimedia Systems are currently being the subject of intense study. Different network technologies capable of supporting efficiently such systems are being analysed to determine which one offers better performance. The Broadband Integrated Service Digital Network (B-ISDN) based on the Asynchronous Transfer Mode (ATM) is one of these candidates. ATM networks provide different service categories [ITU96] to support multimedia services. The applications select a service category based on

[1] This work has been supported in part by the Spanish Science and Technology Commission (CICYT) under grant TIC96-0680

their QoS requirements.

The ABR class of service was initially conceived to support data traffic. Its service model is based on the *best-effort* paradigm but enhanced by some specific characteristics: *fair sharing of the available resources among the contending ABR connections* and *a closed-loop feedback mechanism.*

Video-based applications that are rate adaptive, can obtain substantial benefits by using ABR connections. These benefits can be summarised in the following three aspects. First, these applications typically require some guarantee on bandwidth, for example a minimum encoding rate for a video stream, but can take advantage of spare bandwidth. This can be supported by an ABR connection by defining a Minimum Cell Rate at connection set up. Second, when explicit rate feedback is used and the ABR connections supporting these applications are multiplexed on a dedicated queue at the switches, the cell transfer delay is more predictable because the congestion control mechanism keeps the queues almost empty. And third, the feedback mechanism keeps each source informed of the available bandwidth it has at their disposal. This information can be used by the quantizier to adapt quickly to new network conditions [JMG98]. But, when a video signal that has been processed by a typical video compression standard algorithm, is transmitted over an ABR connection, it is difficult to obtain the best visual quality, as perceived by a human viewer, as we will see in section 2. We take a new approach to solve this problem by designing an adaptive video compression algorithm specific for ABR connections.

The usage of visual criteria is still an open question and different studies can be found in the literature. For example [Che96] introduces a 3D subband coding (with Haar and 16-QMF filters) which uses a Just Noticeable Distortion criteria for 64 Kbps wireless channels. This approach differs from the one described in this paper because, first it uses constant bit rates

rather than ABR services and second, it uses QMF filters which are difficult to implement if linear phase response, similar to the HVS, is required. [Rei97] proposes an optimization technique for adaptive quantization of image and video under delay constraints for ATM VBR connections. In this case, the study focuses on the Rate-Control as an optimal Trellis-based buffered compression, where the Distortion is computed using Mean Square Error measures, which is not related to the HVS.

The rest of the paper is structured as follow. Section 2 describes an experiment in which a H.263 video sequence is transmitted over an ABR connection subjected to different kinds of perturbations. Section 3, proposes a new compression technique using subband decomposition, which is based on the Wavelet Transform(WT) instead of on the DCT(Discrete Cosine Transform) used in: H.261, H.263, MPEG-1, MEPG-2, etc. After the decomposition, a bit allocation is performed based on two limiting factors: HVS perception requirements and available bandwidth on the network. Section 4 describes the operation of the coder. Section 5 evaluates the performance of the proposed compression technique and provides numerical results. Finally, section 6 presents the conclusions and ideas for future work.

2 Performance evaluation of a H.263 video transmission system over an ABR connection

This section evaluates by simulation how an H.263 video signal degrades when it is transmitted over a connection offering a *best-effort* service. The degradation of the video signal will be measured by computing its Signal to Noise Ratio (SNR) and by simple visual perception of the received frames. This experiment highlights the fact that a quantitative performance parameter like the SNR is not always linearly related to the perceived human quality.

2.1 Reference Network Configuration

The network configuration used in the experiment can be observed in figure 1. As can be seen, it is a simple two node configuration in which all the connections have their bottleneck at the same link (D11). This link is the backbone link. Source A has just one connection set up with destination A and this connection is supporting the H.263 video signal. The other connections are ABR connections supporting greedy sources, that is, sources that will use as much bandwidth as it available for them.

The capacity of the access links, as well as the capacity of the backbone link, is 10 Mbps. The length of the access links is 0.2 Km, while the length of the backbone link is 2 Km. The ABR switch algorithm used is an improved version of the CAPC algorithm as described in [JMG98]. The values used for the source parameters and for the switch parameters have also been taken from [JMG98].

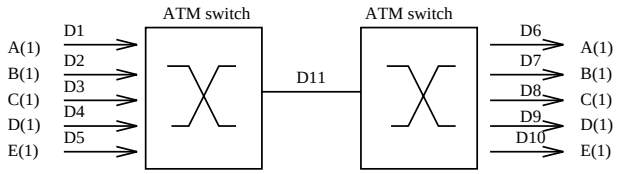

Figure 1: *The network configuration with 2 ATM switches*

As the objective of the experiment is to stress as much as possible the video signal, two major disturbances have been introduced in the experiment. The first one takes place at 400 ms and emulates the set up of a new connection that consumes a bandwidth of 5 Mbps. The second one takes place at 900 ms and emulates the set up of new connection that consumes an additional portion of 3 Mbps. These events could emulate, for example, the set up of two CBR connections with different Peak Cell Rates. Also, multiplexing greedy sources on the same bottleneck link used by the video connection ensures that the video connection will have to contend for bandwidth, and it will never get more than its fair share.

Given that the capacity of the backbone link is 10 Mbps ($23.58\frac{cells}{ms}$) and that there are 5 ABR connections sharing this capacity, each connection has ($\frac{23.58}{5} = 4.71\frac{cells}{ms}$ available during the first 400 ms. The video coder uses a Source Input Signal (SIF) format of 352x288 pixels and, therefore, requires a compression rate of 11.55:1 during this time interval. The compression ratio required during the 400 to 900 ms interval is 23.10:1 and 57.77:1 after 900 ms. The Minimum Cell Rate for the video source has been set to 360 Kbps which ensures that the compression rate will never be lower than 64:1.

2.2 Results of the Experiment

The most common compression technique used by video standards is motion estimation with DCT. This technique is also used by the ITU-T H.263 recommendation. Figure 2 describes the basic functional blocks diagram of a video coder: motion estimation, DCT, quantization and entropy coding. As can be observed, the quantization step can be changed by a external signal. Basically, this external signal controls the rate of the video signal at the output of the coder. During the experiment we have made use of this control signal to make sure that the video coder output rate is always consistent with the bandwidth that the connection has available.

A H.263 video coder generates a hierarchical data structure. This structure introduces frame dependencies as can be seen in figure 3, where *I intra-frames* are independent ones, *P predictive-frames* are dependent on the I frame and *B bidirectional-frames* are dependent on the I and P frames.

When using this type of video coder in a scenario where the available bandwidth is not constant and cell losses can occur, different kind of problems can appear. First, the hierarchical frame structure based on motion estimation makes possible the propagation of

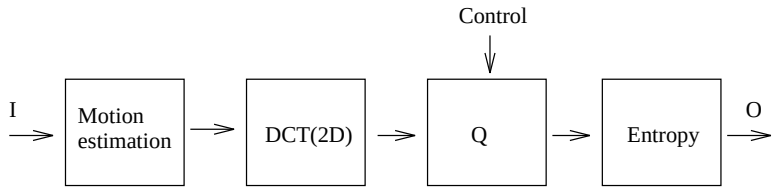

Figure 2: *Functional block diagram of a video coder based on motion estimation and DCT*

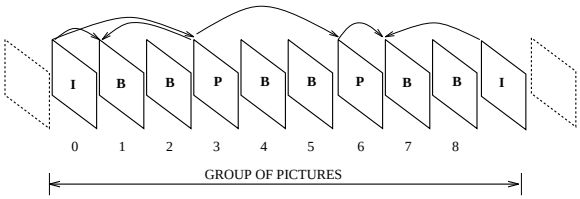

Figure 3: *Group of pictures and the dependences among I intra-frames, P predictive-frames and B bidirectional-frames*

errors. Second, the DCT does not operate in the same way as the HVS, under very low bit rates [SN96], then video perception that a viewer has is unpredictable. And third, the mosquito noise due to the rigid 8x8 pixel block size [SN96].

Figure 4 shows three frames of the H.263 sequence under evaluation. The selection of these three frames have been done as follows. The first one corresponds to the frame that was being transmitted by the source when the first bandwidth reduction took place at 400 ms. The second one corresponds to the frame that was being transmitted by the source when the second bandwidth reduction took place at 900 ms. And the third is a frame selected at random when the source was using the smaller bandwidth portion, that is, after 900 ms.

The SNR (db) for each of the three frame is: 36.82, 15.2 and 32.82 (from left to right). As can be observed, the quality perceived from the second frame cannot be anticipated by its SNR value.

Finally, it should be pointed out that the H.263 coder used does not implement any type of progressive transmission method to improve the quality of the received signal[RH96],

because as previously discussed, under low bit rates, it still works in a bad way.

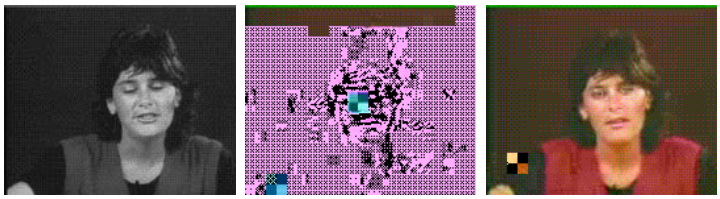

Figure 4: *The three selected frames from the Miss America sequence as perceived at destination*

3 The Proposed Adaptive Video Compression Algorithm

Video images have a lot of spatial, frequential and temporal redundancy, besides the subjective redundancy. To take advantage of this redundancy different techniques have been proposed to reduce the bandwidth required to transmit a video signal. Subband coding methods have a better response when the signal has to be transmitted over networks that offer *best-effort* services.

In these network scenarios, the best choice, as it will be shown, is to mimic the behaviour of the HVS. This paper proposes to mimic the HVS in two ways: first by performing a multiresolution decomposition of the video signal using a WT[Wat87] and second, by introducing a visual criteria to help the coder to determine which subbands need a prioritized treatment. As it will shown, a subband with higher priority will get more bits allocated and will be transmitted earlier. The perceptual criteria used for the experiments described in this paper is the one presented in [Art97]. Figure 5 shows a functional block diagram of the proposed video coder. Notice, that in figure 5, the quantization step can also be modified by the control input.

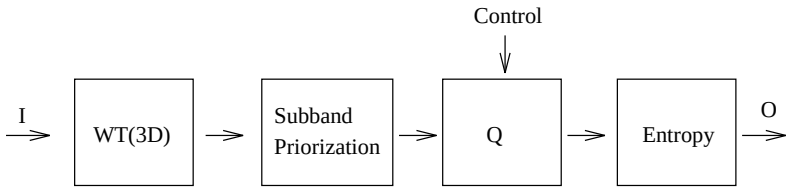

Figure 5: *Functional block diagram of a the proposed video coder based on the Wavelet Transform*

One of the objectives of performing a decomposition in a 3D domain is to achieve a frequency response that is approximately constant logarithmic, similar to the HVS[Wat87]. In the proposed system, this decomposition is done by splitting each frequency domain (horizontal, vertical and temporal) into two parts, as can be seen on the left of figure 6. By this process we get 2x2x2 frequency shares (called subbands) that compose the first resolution level. If the absolute low pass subband (from the output of every low-pass filter of each domain), is processed again, we get 2x2x2 subbands more, that compose the second resolution level.

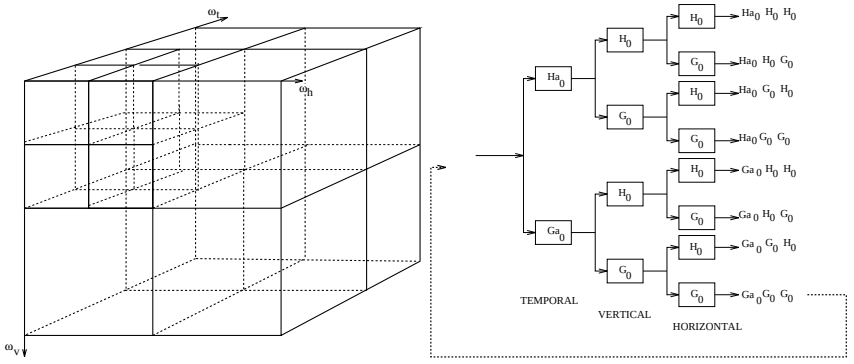

Figure 6: *Left: Frequency division for the horizontal, vertical and temporal domains into two resolution levels using a 3D dyadic separable WT. Right: Its filter bank implementation.*

The right side of the figure 6 shows a fast separable 3D WT decomposition using recursive biorthogonal filter banks, where the high-pass is called *wavelet function* or filter G, and the low-pass is called *scaling function*, or filter H. As can be observed, the second resolution level

is obtained by a new iteration, where the absolute low pass subband is feedback as a new input to the filter bank. The output of each filter is undersampled by 2 (dyadic sampling) to keep constant the amount of information[Vai93], without adding any redundancy.

The notation that will be used to identify each subband is: t and T for the temporal low and high responses, h and H for the horizontal low and high responses and v and V for the vertical low and high responses.

To perform the inverse transform the same filter structure is used in reverse mode but changing the analysis filters by synthesis filters. Both the analysis and synthesis filters have to meet the following requirements: perfect reconstruction, null aliasing and null distortion[SN96][Vai93]. These biorthogonal filters have been designed to be linear, using Daubechies' method, avoiding in this way damaging the image after the quantization process [SN96]. It should also be noticed that a 2 coefficient filter (Haar filter) have been used in the temporal axis to reduce the number of frames that need to be stored by the coder. These filters are labelled with subindex a_0 in figure 6.

The transfer functions of the analysis (with subindex $_0$) and synthesis (with subindex $_1$) filters, both for the horizontal and vertical domains, are:

$$\begin{aligned} H_0(z) &= \tfrac{1}{4}(1+2z^{-1}+z^{-2}) & H_1(z) &= \tfrac{1}{4}(-1+2z^{-1}+6z^{-2}+2z^{-3}-z^{-4}) \\ G_0(z) &= \tfrac{1}{4}(1+2z^{-1}-6z^{-2}+2z^{-3}+z^{-4}) & G_1(z) &= \tfrac{1}{4}(1-2z^{-1}+z^{-2}) \end{aligned} \tag{1}$$

4 Operation of System

When a system with two resolution levels, as the one described in the previous section, is fed with a video sequence of 25 $\frac{frame}{sec}$, then a set of 4 frames (4x40=160 ms) are needed to perform a complete 3D decomposition. This represents a trade off between the decorrelation

ratio and the number of frames that need to stored at the coder. The process can be observed in figure 7.

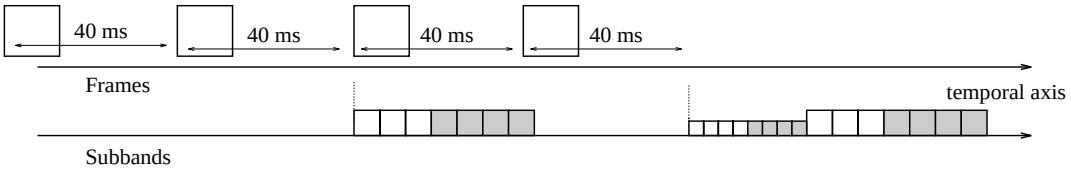

Figure 7: *Subband generation using 3D Wavelet Transform with two resolution levels. Different frames are processed every 40 ms*

For example, lets assume that our system is going to perform the decomposition of 4 frames, that we label as frames 1, 2, 3 and 4. The system uses the pair of frames 1-2 and the pair 3-4 to obtain the first resolution level. This process generates 8 subbands from each pair of frames. Then we use the pair of subbands *tvh* from each of the original pair of frames (1-2 and 3-4) to generate the second resolution level. By this process we obtain 8 additional subbands. Therefore, at the end of the decomposition process we obtain 7+7+8 subbands [2]. The absolute low pass subband (or *tvh*) of the second resolution level is coded using Differential Pulse Code Modulation (DPCM) because it has a uniform pixel distribution.

In figure 7, the white boxes represent subbands with low temporal frequencies while the dark boxes represent subbands with high temporal frequencies. For an example of the 8 subbands from the second resolution level of Miss America, see figure 8.

After this decomposition, the Bit Allocation Algorithm estimates the number of bits per coefficient (or the total number of bits for each subband). The Bit Allocation Algorithm requires two inputs: the bandwidth that the connection has available at any point in time and the priority of the subband, being the later obtained by applying the visual criteria.

[2]Note, that the 2 low pass ones of the first resolution level (denoted *tvh*) have been used for the second resolution and will not be transmitted.

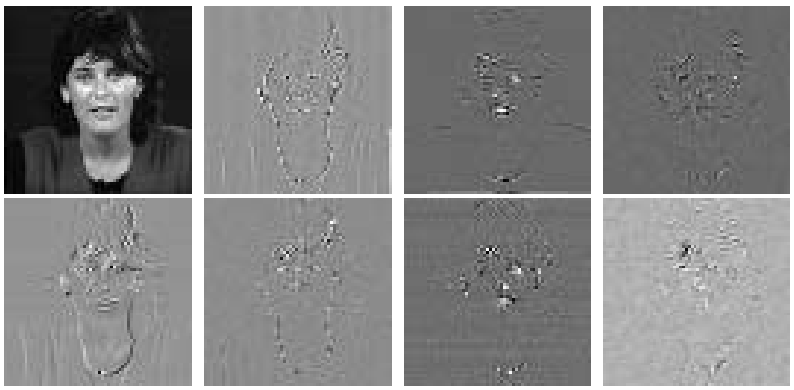

Figure 8: *Subbands from the second resolution level of Miss America. ¿From top to bottom and from left to right: tvh, tvH, tVh, tVH, Tvh, TvH, TVh and tVH*

4.1 Estimation of the Connection Available Bandwidth

An ABR connection receives periodic information from the network of the bandwidth it has available. This information is conveyed by a special type of cells called Resource Management (RM) cells. The RM cells are inserted by the source in the normal data cell flow sent toward the destination terminal. Once the RM cells get to the destination terminal then they are sent back to the source, collecting on their way congestion state information supplied by the switches.

The transmission rate of an ABR source is computed by taking into account both the information conveyed by the RM cells and a set of source behaviour rules [Kim96]. The rate at which an ABR source can transmit at any given time is called *Allowed Cell Rate* (ACR). The proposed video coder tracks the values taken by the ACR to estimate the bandwidth that a connection has available.

The value of the ACR changes in a very small time scale (in the order of hundreds of μs) and cannot be used directly by the coder. Bear in mind that the coder works at the frame time scale [3], therefore it only requires to estimate the connection available bandwidth

[3] In fact, the proposed coder works at a time scale equivalent to four frames (160 ms) according to the

at this time scale. This can be achieved by filtering the values taken by the ACR. One technique that is easy to implement is to perform an exponential weighted averaging of the ACR samples, that is $MACR = MACR + \alpha(ACR - MACR)$, where MACR (Mean ACR) is the estimated available bandwidth and α determines the cut-off frequency of the low pass filter. The value of α can be related to the sampling frequency by

$$\cos w_c = \frac{\alpha^2 + 2\alpha - 2}{2(\alpha - 1)} \tag{2}$$

One of the problems to determine the value of α is that the sampling frequency is not constant. It depends on the inter-arrival times of the RM cells, which itself is a function of the available bandwidth that changes with time. A common trade-off value is $\alpha = \frac{1}{16}$

The video coder uses the value of MACR as a forecast of the bandwidth that the connection will have available during the next 160 ms. Figure 9 shows how the MACR estimator performs during an experiment carried out in the same conditions of the experiment described in section 2, but using the proposed video coder instead of a H.263 coder. The same figure shows how the ACR of the ABR video source adapts to the changing network conditions and the backbone link utilisation factor.

4.2 Bit Allocation Algorithm

The bit allocation procedure is done applying the Rate-Distortion theory. This requires to choose the probability density function of the coefficients in every subband in order to estimate the distortion noise introduced by every quantization process. These pdfs are well characterised by generalised Gaussian distributions with zero mean [SN96]. In general, subbands with lower energy should have fewer bits, but the subbands with more perceptual weight (like the low pass ones) get more bits per pixel.

---

decomposition method descried earlier.

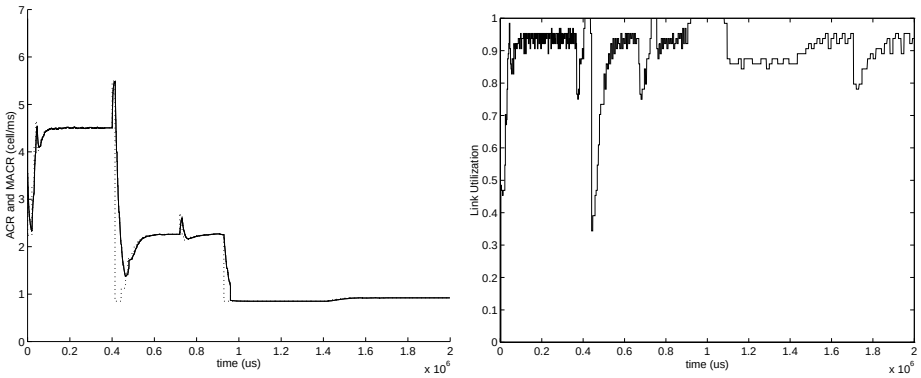

Figure 9: *Left: Evolution of the ACR (dotted line) and of the MACR (continuous line) as a function of time for the H.263 video transmission experiment. Right: backbone link utilisation for the same experiment.*

The Rate-Distortion theory (equations 3 and 4) is based on the computation of the Mean Square Error (MSE) which it is not an HVS mechanism [SN96]. The proposed video coder introduces weighted HVS factors [Art97] to achieve a better perceptual bit allocation. The bit allocation is estimated by minimising the next equations:

$$Distortion: \quad D(b) = \sum_{k=1}^{M} \alpha_k \omega_K c_K 2^{-2b_k} \sigma_k^2 \tag{3}$$

$$Rate: \quad R(b) = \sum_{k=1}^{M} \alpha_k b_k \leq 4 * \frac{(MACR) * 48 * 8}{N * f_{rate}} = R \tag{4}$$

where M is the number of processed subbands (in our case 7+7+8), N is the total number of pixels available (in our case the number of pixels within 4 frames), $MACR$ is the forecasted available bandwidth, $f_{rate} = 25\ \frac{frame}{sec}$, c_k is a pdf coefficient, α_k is the relative subband size, $b = (b_1, b_2, ..., b_M)$ represents the bit per coefficient for each subband, σ_k^2 is the subband variance and ω_K is the weighted HVS factor.

By the Lagrange theorem we can minimise D(b) given R(b), by finding $\min(D(b)+\lambda R(b))$ where $\lambda' = \frac{\lambda}{c_k}$ and then

$$b_k = 0.5 * \log_2(\frac{2\ln(2)\omega_k \sigma_k^2}{\lambda'}) \quad \text{with} \quad \lambda' = 2^{\frac{\left[\sum^{22} \alpha_k (\log_2(2\ln 2) + \log_2(\omega_k \sigma_k^2)) - 2*R\right]}{\sum^{22} \alpha_k}} \tag{5}$$

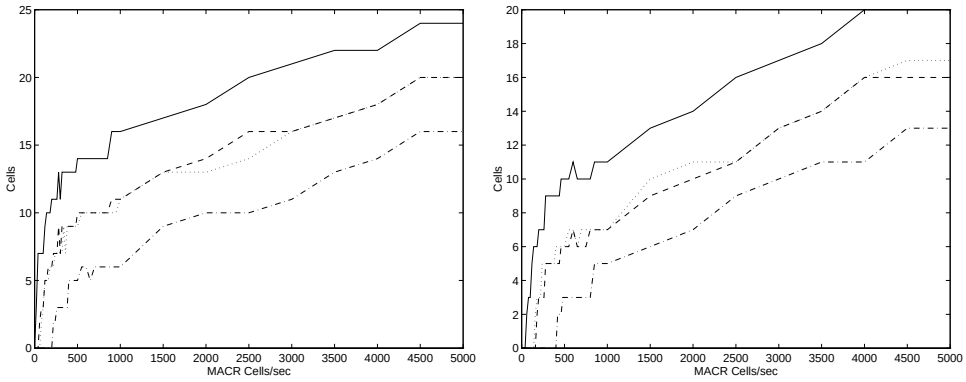

Figure 10: *Bit allocation algorithm results: Number of cells for each subband of the second resolution level. Subband identification: i) Left: tvh (solid), tvH (dashed), tVh (dotted) and tVH (dash-dot). ii) Right: Tvh (solid), TvH (dashed), TVh (dotted) and TVH (dash-dot)*

Assuming the maximum absolute coefficient value as four times the standard deviation [SN96], we can get the quantization step and the number of cells required for every subband. The bit allocation algorithm is executed every 4 frames (160 ms) and it takes the value that MACR has at that time.

Figure 10 plots the number of cells required for the 8 subbands of the second resolution level, as a function of MACR. If a subband has no bit allocated to it, an infinite quantization step is assumed and no information will be transmitted for it.

4.3 Adaptation to the Service Provided by the Network

Once the information generated by each subband is available, the coder creates an information unit per subband; each information unit contains: the frame number, subband number, and the quantization step. The information unit just described forms, what in ATM jargon is called the *Service Specific Convergence Sublayer* Packet Data Unit (SSCS-PDU). This PDU is then transferred to the *Common Part Convergency Sublayer* (CPCS), where it is

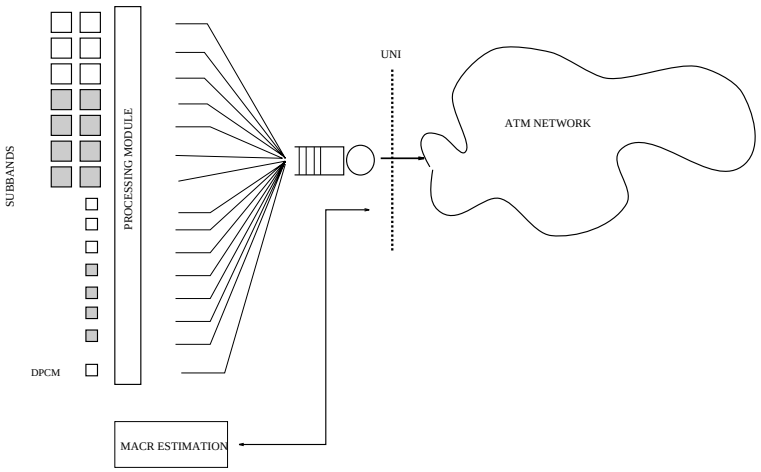

Figure 11: *Functional block diagram of the transmission subsystem: Processing Module, Transmission Buffer and MACR Estimation.*

encapsulated in a CPCS- PDU and then segmented by the Segmentation and Reassemble (SAR) sublayer. In this study we have used the ATM Adaptation Layer 5 which CPCS-PDU format is defined in [AAL93].

The order in which the different SSCS-PDUs get transferred to the CPCS will define the order in which the different subbands will be transmitted. This order is determined by their perceptual priority, which is related to their energy and to the HVS criteria selected. Once the subbands have been ordered, the highest priority subband is transmitted first. This ordering mechanism can be observed in figure 11.

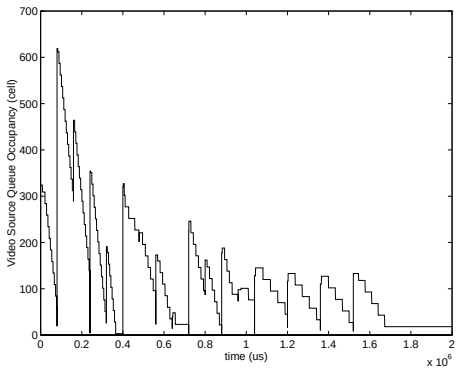

Figure 12: *Queue occupancy at the video transmission system*

The available bandwidth forecast computed by the video coder can be sometimes too optimistic. In this cases, when a new set of subbands arrive to the ATM layer ready for transmission, any stale information must be flushed. In general, this queue flushing mechanism will only deteriorate minimally the quality because it will only affect the low priority subbands. An evolution of the queue occupancy can be seen in figure 12. Again, this has been taken from an experiment carried out in the same conditions of the experiment described in section 2, but using the proposed video coder instead of an H.263 coder.

5 Performance evaluation of the proposed video coder over an ABR connection

To evaluate the performace of the proposed video coder the experiment described in 2 has been repeated here in exactly the same conditions. The results can be observed in figure 13. In this case, the SNR(db) of the three selected frames are: 37.10, 35.7 and 31.4. As can be seen, the perceived visual quality is better now.

Figure 13: *Three different frames from Miss America sequence using the adaptive compression system. The first three are at next simulation transitions: switch from 10 to 5 Mbps, switch from 5 to 2 Mbps and finally at 2 Mbps*

A new set of experiments have been carried out to evaluate the percentage of transmitted frames that are received successfully at destination. By successfully received frames we mean both the frames that have arrived with no errors and the frames that have arrived on time.

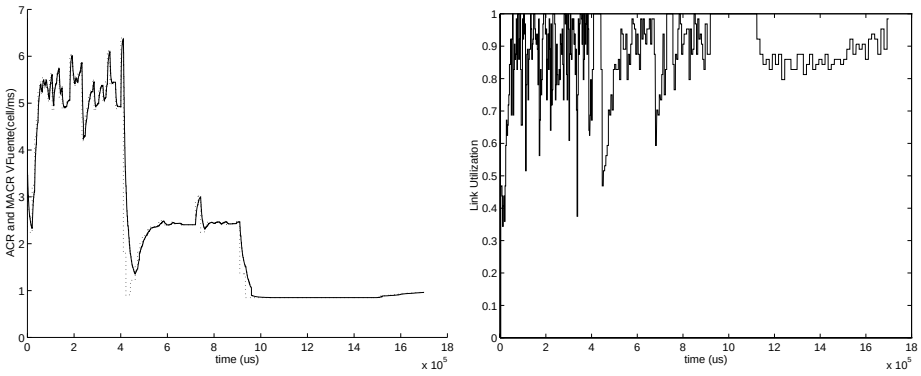

Figure 14: *Left: ACR (dotted line) and MACR (continuous line). Right: Backbone link utilisation.*

A frame arrives on time when its end-to-end transfer delay is less than 21 ms. This value has been chosen by observing the peak queue occupancy at the switch output port attached to the bottleneck link. Each one of these experiments has been performed in exactly the same scenario described for the experiment of the section 2, but this time the ABR data connections have a bursty traffic profile instead of being greedy sources. For simplicity, both the burst lengths and the inter-burst intervals have been generated randomly, but with such probability to keep every bursty source with a mean cell rate of $6.28\frac{cell}{ms}$, with burst lengths of 2, 16 and 32 cells.

For the 8 subbans of the second resolution level, the results are shown in Table 1. The values represent the successful arrival probability conditioned to the fact that the subband under consideration has been transmitted. As can be observed, the successful arrival probability of the most important subbands is quite high, which insures a good reception quality even under very demanding network scenarios. Figure 14 shows how the ACR, the MACR and the backbone link utilization factor change with time during one of the experiments.

subband	$\hat{P}(C/T)$	*subband*	$\hat{P}(C/T)$
tvh	0.9900	Tvh	0.8142
tvH	0.9495	TvH	0.7347
tVh	0.9011	TVh	0.7426
tVH	0.8542	TVH	0.7663

Table 1: *P(C/T) for the 8 subbands of second resolution level*

6 Conclusions and future work

This paper shows that the successful transmission of video over connections that only offer a *best-effort* service is possible. In spite of the lack of QoS assurances, the proposed video compression algorithm can offer a good adaptive response when used over ABR connections.

The proposed coder tries to maintain the *subjective quality constant* by minimizing the loss probability for the subbands that carry the relevant part of the information. This is achieved by prioryzing the transmission of the subbands according to the weight assigned to them by the perceptual criteria used and by observing the ABR source behaviour rules. The ABR service guarantees that sources which obey the feedback signal supplied by the network will achieve low losses.

Future work should be oriented towards designing an enhanced ABR switch algorithm. This algorithm should be able to guarantee that the important subbands will never be lost.

References

[AAL93] Rec. i363 b-isdn atm adaptation layer spec. *ITU-T*, 1993.

[Art97] J. Malo A. Pons A. Felipe J. Artigas. Characterization of the human visual system threshold performance by a weighting function in the gabor domain. *Journal of*

Modern Optics, 44(1):127–148, 1997.

[Che96] C Chou C Chen. A perceptually optimized 3d subband codec for video communication over wireless channels. *IEEE Trans. on Circ. and Syst. Video Tech.*, 1996.

[ITU96] Rec. i371 traffic control and congestion control in b-isdn atm. *ITU-T*, May 1996.

[JMG98] J.R. Vidal J. Martinez and L. Guijarro. A low complexity congestion control algorithm for the abr class of service. In *IDMS98*, pages 219–230, September 1998.

[Kim96] R. Jain S. Kalyanaraman S.Fahmy R. Goyal S. Kim. Source behavior for atm abr traffic management: An explanation. *IEEE Communications Magazine*, 34:50–57, November 1996.

[Rei97] Chi-Yuan Hsu A. Ortega A. Reibman. Joint selection of source and channel rate for vbr video transmission under atm policing constraints. *IEEE Journal on Selected Areas in Commun.*, 1997.

[RH96] K. R. Rao and J. J. Hwang. *Techniques and Standards for Image , Video and Audio Coding*. Signal processing series. Prentice Hall, New Jersey, 1996.

[SN96] Gilbert Strang and T. Nguyen. *Wavelets and Filter Banks*. Wellesley-Cambridge Press, USA, 1996.

[Vai93] P. P. Vaidyanathan. *Multirate systems and filter banks*. Prentice Hall, 1993.

[Wat87] A. B. Watson. Efficiency of a model human image code. *Journal of the Opt. Soc. of Am.*, 1987.